

PROCEEDINGS OF SPIE

[SPIDigitalLibrary.org/conference-proceedings-of-spie](https://spiedigitallibrary.org/conference-proceedings-of-spie)

External coupling and cathode effects in organic light-emitting devices: modeling and experiments

Min-Hao Lu, James C. Sturm

presented July 30-Aug 1, 2001

Min-Hao Lu, James C. Sturm, "External coupling and cathode effects in organic light-emitting devices: modeling and experiments," Proc. SPIE 4464, Organic Light-Emitting Materials and Devices V, (27 February 2002); doi: 10.1117/12.457475

SPIE.

Event: International Symposium on Optical Science and Technology, 2001, San Diego, CA, United States

External coupling and cathode effects in organic light-emitting devices: modeling and experiments

M.-H. Lu* and J. C. Sturm**, Center for Photonics and Optoelectronic Materials, Department of Electrical Engineering, Princeton University

ABSTRACT

The emission of light and the external coupling after appropriate excitons have been formed in the organic light-emitting devices have been investigated. A combined classical and quantum mechanical model was used to calculate the distribution of the internally emitted light into the externally emitted and various waveguided modes in an organic light-emitting device on planar substrates. The exciton lifetime in the OLED cavity was calculated by a Green's function formalism, with a focus on the non-radiative energy transfer to the cathode. Various efficiency measures as a function of the thickness of the indium-tin-oxide anode were calculated and the numerical results were in agreement with the measured external quantum efficiencies.

Keywords: organic light-emitting devices, out coupling

1. INTRODUCTION

Recently, organic light-emitting diodes (OLEDs) have attracted wide interest, primarily due to their applications in flat panel displays while their use for general lighting is also being considered. One critical figure of merit for OLEDs is the electroluminescence (EL) efficiency, η_{EL}^{ext} (externally emitted photons/electron). Usually it is written as the product of the internal quantum efficiency, η_{EL}^{int} (internally emitted photons/electron), and the external coupling efficiency, η_{cp}^{ext} , the fraction of thus internally emitted photons that actually escapes to the viewer. In this paper, we use a combined classical and quantum mechanical microcavity (CCQMM) model to investigate the emission of light after appropriate excitons have been formed in the OLED. The effect of various cathode materials on the exciton lifetime and various efficiency measures and their dependencies on the OLED structure are calculated. The numerical results are compared with the experimental data from OLEDs with varying thickness of the indium-tin-oxide (ITO) anode.

2. THEORY

2.1 OLED structure

A schematic diagram of the OLED structure used in both modeling and experiments is shown in Figure 1. The device consists of a soda lime glass substrate ($n_{\text{glass}} = 1.51$), an ITO ($n_{\text{ITO}} = 1.8$) anode, a poly-(N-vinylcarbazole) (PVK, $n_{\text{PVK}} = 1.67$) hole transporting layer, a tris-(8-hydroxyquinoline) aluminum (Alq_3 , $n_{\text{Alq}_3} = 1.71$) electron transporting and emitting layer, and a 30-50 nm Mg:Ag (10:1) cathode followed by a 150 nm Ag cap. The electroluminescence (EL) spectrum shows that the emission comes exclusively from the Alq_3 layer. The OLED microcavity is confined by the reflecting cathode and the leaky ITO/glass interface.

The emitted light can be classified into three modes: the external modes which escape the substrate, the substrate-waveguided modes which are trapped in the glass substrate by total internal reflection (TIR) at the glass/air interface, and the ITO/organic-waveguided modes which are trapped by TIR at the ITO/glass interface (Figure 2).

* Currently with Universal Display Corporation, mlu@universaldisplay.com; phone 1 609 671-0980x252; fax 1 609 671-0995; 375 Phillips Blvd., Ewing, NJ, USA 08618

** sturm@ee.princeton.edu; phone 1 609 258-5610; fax 1 609 258-1954; E-Quad, Olden St., Princeton, NJ USA 08540

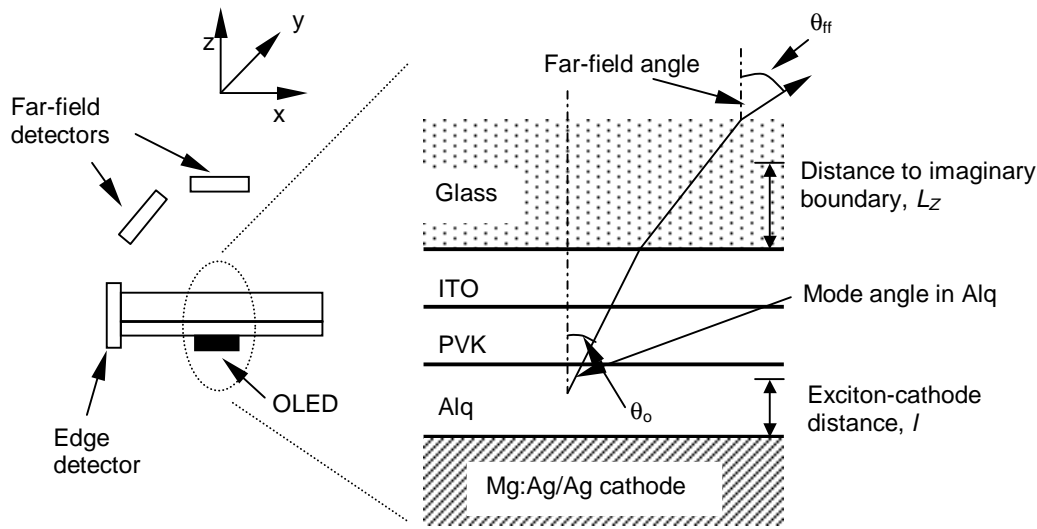


Figure 1 Schematic diagram of the setup for modeling and experiments.

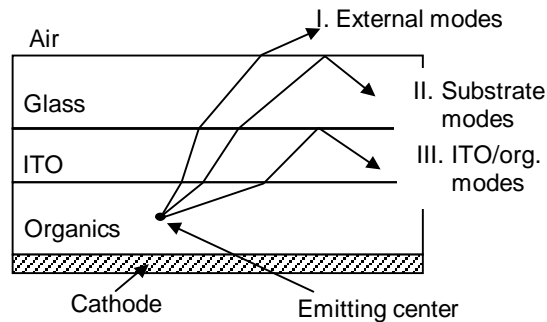


Figure 2 Three radiative modes in OLEDs: I. External modes, II. Substrate modes, and III. ITO/organic modes.

2.2 Background

In a planar OLED, a large fraction of the light is lost to waveguiding modes in the glass, ITO and organic layers due to index mismatching. This effect is well known in inorganic semiconductor light emitting diodes, where the external coupling efficiency is estimated by classical ray optics to be $1/2n^2$ for large n .^{1, 2} However, classical ray optics is ill-suited for describing the thin multi-layers of an OLED. The ray optics result leads to unrealistically high estimates for the internal quantum efficiency in some efficient devices.^{3, 4} In addition, several groups have reported dependence of the far-field emission pattern on the thickness of the organic layer, which is not explained by the classical theory.^{5, 6}

The behavior of radiating molecules in an optical microcavity is a general problem that can be approached in two ways: one based on classical electrodynamics and one based on quantum mechanics.⁷⁻²² Among them, the most complete treatment is that of Chance, Prock, and Sibley,¹⁴ where the radiating molecule is modeled as a classical oscillating dipole and the radiation fields in the layered media is described by a dyadic Green's function formalism. Some of their earlier work was based on a

* Assuming the emitting organic layer is a Lambertian source, the external coupling efficiency is calculated to be $1/n^2$ using ray optics; however, there does not appear to be an *a priori* justification for this assumption. The emission profile of most OLEDs follows a modified cosine distribution: deviating slightly from a Lambertian profile.^{13, 23} At any rate, it seems most natural to consider the collection of emitting molecules an assemblage of individual point sources.

Hertzian vector approach that has recently been applied to OLEDs by Kahen.¹⁵⁻¹⁷ It has been shown that the Green's function method is completely equivalent and more easily applied to general stratified media.¹⁴ A simpler version of this theory has been used to explain photoluminescence data from an Alq₃-Al system.¹⁸

A combined classical and quantum mechanical (CCQMM) model was developed by Bulovic et al.²² In the QM treatment, the electromagnetic field in the layered microcavity is represented by the sum of eigenmodes of the cavity; the radiating molecule is modeled as a dipole; and the transition probability into each mode is given by Fermi's golden rule. It has the advantage that the transition rates into the external, substrate and ITO/organic modes are computed separately. The shortcoming of the quantum mechanical approach is that it does not account for the energy transfer from the dipole to the metal electrodes. However, it was shown by Chance et al. that this energy transfer arises exclusively from the near field of the dipole,¹⁴ so it does not affect the shape of the normalized far-field intensity patterns. In the model developed by Bulovic et al., the QM microcavity treatment is augmented by the Green's function analysis which is more convenient in computing the total rate of energy loss, hence the dipole lifetime in layered media.²² We will use this model to determine the distribution of luminous flux emitted into the three above-mentioned modes and to examine its dependence on the thickness and material constants of the constituent layers.

2.3 The exciton recombination process

Both electroluminescence and photoluminescence (PL) are due to the radiative recombination of Frenkel excitons within the organic layers.²⁶ Since the quantum mechanical approach is based on the dipole approximation, and the classical analysis models the recombining excitons as oscillating dipoles we will use the terms "exciton" and "dipole" interchangeably. A schematic diagram of the emission process is shown in Figure 3. Our discussion is based on the emitter/electron transport material, Alq₃, but can be easily extended to doped or electrophosphorescent devices. For example, the set of path occurring under "singlets" in Figure 3 could easily be applied to "triplets" as well.

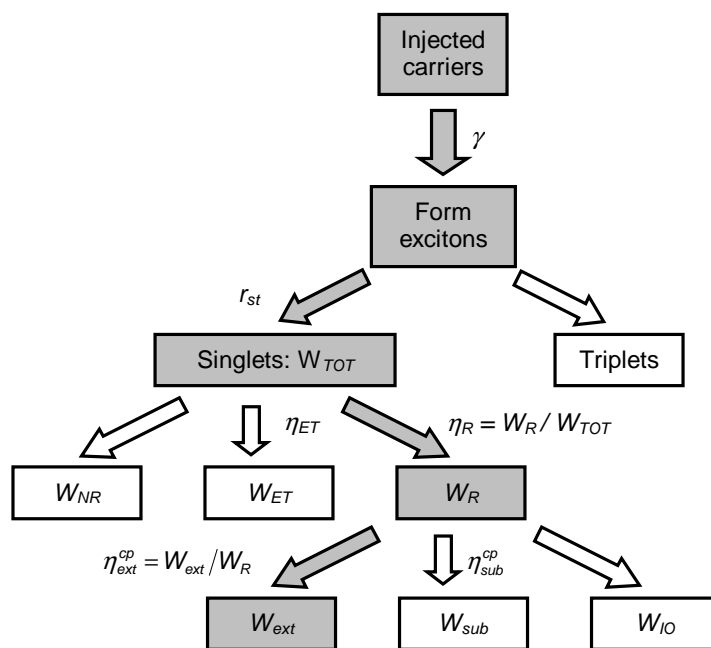


Figure 3 A schematic diagram of electrofluorescence in OLEDs: the gray path indicates the mechanism by which useful EL is emitted.

For each electron injected into the device, a fraction of γr_{st} results in singlet excitons, where γ is the number of exciton forming events per electron flowing through the OLED, and r_{st} is the fraction of singlet excitons. The decay of the singlet excitons is described by the following equation:

$$\begin{aligned} W_{TOT} &= W_R + W_{ET} + W_{NR} \\ W_R &= W_{ext} + W_{sub} + W_{IO} \end{aligned} \quad (1)$$

where W_{TOT} is the total rate of decay of the singlet excitons. The rate of radiative decay, W_R , is the sum of the decay rates of the external, substrate and ITO/organic modes. W_{ET} denotes the rate of energy transfer to the metallic cathode via non-radiative dipole-metal transfer and excitation of surface plasmons. W_{NR} denotes the rate of non-radiative decay of the exciton which is assumed to be unaffected by the placement in the microcavity, thus $W_{NR} = W_{NR}^0$. W_{NR}^0 is the intrinsic rate of non-radiative decay due to internal conversion and intersystem crossing which can be calculated from the photoluminescence quantum efficiency, η_{PL} , of a thick film:²²

$$\eta_{PL} = W_0 / (W_0 + W_{NR}^0), \quad (2)$$

where W_0 is the intrinsic rate of radiative decay. η_{PL} of Alq₃ has been accurately measured to be $32 \pm 2\%$, or $W_{NR}^0 = 2.125W_0$.²⁷ The fraction of internally generated photons that are emitted externally is given by the external coupling efficiency:

$$\eta_{cp}^{ext} = W_{ext} / W_R, \quad (3)$$

which is commonly held to be $\sim 20\%$ by ray optics, a figure that we will revisit later. Also of great interest is the number of photons emitted externally for every singlet exciton created, $\eta_{exciton}$,

$$\eta_{exciton} = W_{ext} / W_{TOT}, \quad (4)$$

which takes the non-radiative decay into account; consequently, it is a better measure of the external emission from the exciton in the microcavity. This can be seen more clearly if we let τ denote the lifetime of the exciton: the amount of radiation each exciton emits into the external modes is then given by $W_{ext} \tau \propto W_{ext} / W_{TOT} = \eta_{exciton}$. Various efficiency measures are related to each other as follows (Figure 3)

$$\begin{aligned} \eta_{EL}^{ext} &= \eta_{EL}^{int} \eta_{cp}^{ext} = \gamma r_{st} \eta_{exciton} \\ \eta_{EL}^{int} &= \gamma r_{st} \eta_R \\ \eta_{exciton} &= \eta_R \eta_{cp}^{ext} \end{aligned} \quad (5)$$

It can be seen from eq. (5) that the exact value of $\eta_{exciton}$ as a function of the emitter location in the cavity is critical in extracting the ratio of singlet/triplet excitons.^{13, 28}

Backside substrate patterning has been shown to increase the external emission by converting some of the substrate modes into external modes.²³⁻²⁵ This conversion can be accounted for by replacing W_{ext} with $(W_{ext} + \beta W_{sub})$ in eqs. (3) and (4), where β is the conversion efficiency.

2.4 Microcavity effects

Both the radiative modes and the dipole-cathode energy transfer are derived from the electric fields of the dipole. The difference is that the radiative modes arise from the far-field and the dipole-cathode energy transfer from the near-field. Both are affected by the OLED microcavity. Therefore, optimization of the external coupling efficiency requires maximizing the appropriate radiative modes and minimizing the dipole-cathode energy transfer. $\eta_{exciton}$ as defined takes into account both radiative modes and the dipole-cathode energy transfer, so optimizing the OLED external coupling efficiency amounts to optimizing $\eta_{exciton}$.

2.4.1 Radiative modes

The decay rate into the radiative modes are calculated using a QM approach where the exciton is modeled as a two-level system whose transition rate is given by Fermi's golden rule. The decay rate is weighted by the PL spectrum of the emitter (an indicator of the oscillator strength) and the exciton recombination profile in the OLED cavity. The details are presented

elsewhere.^{24,42} The intensity of each mode is proportional to the square of the magnitude of the electric field at the location of the emitter. The thickness of the OLED is such that normally there is only one maximum (antinode) in the electric field in the organic layer. Assuming the cathode is a perfect metal, there is a node in the electric field at the cathode and the first antinode is located a quarter wavelength away from the cathode, which for Alq₃ (peak wavelength = 524 nm) is approximately 77 nm (Figure 4).

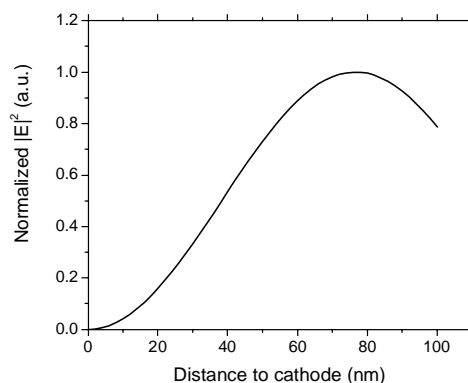


Figure 4 Normalized square of the magnitude of the electric field (proportional to the intensity of the mode) vs. distance to cathode in the organic layer. The wave vector is in the normal direction. The OLED cavity has the structure: cathode (perfect metal)/organics ($n = 1.7$, $t = 150\text{nm}$)/ITO ($n = 1.8$, $t = 120\text{ nm}$)/glass ($n=1.51$). Calculated for a monochromatic emitter at 524 nm.

2.4.2 Energy transfer to the cathode

In this section we discuss the non-radiative energy transfer that arises from the near-field interaction between the dipole and the metal cathode. The QM microcavity treatment provides an accurate description of the far-field radiative modes, but does not take into account this energy transfer to the cathode which can dramatically increase the total decay rate, W_{TOT} . In the absence of the microcavity, a dipole placed close to a metal surface sees an energy transfer rate in the form of $W_{ET} \propto l^{-3}$ in the limit of short dipole-cathode separation $l \ll \lambda$.¹⁴⁻¹⁶ Although the effect of the cathode is expected to remain preeminent for a dipole in the OLED weak microcavity, the other dielectric interfaces also affect the field distribution in the microcavity; therefore, a more complete analysis is required for an exact solution. We use a Green's function formalism to calculate the normalized decay rates due to the fields of the dipole ($W_R + W_{ET}$)/ W_0 , taking into consideration the complex permittivity of the metal cathode. The readers are referred to Refs. 14 and 33 for detailed derivations. Figure 5 illustrates the calculated decay rate as a function of dipole-cathode distance for a monochromatic emitter at 524 nm placed in a microcavity consists of cathode/organic layer/ITO/glass, where the cathode material is Ag, Al or Mg. At a short distance away, the interaction between the near-field of the dipole and the metal leads to a high W_{ET} , i.e. cathode quenching, resulting in a very short lifetime. The rate of energy transfer is twice as fast for a perpendicular dipole as for a parallel dipole, the physics of which is similar to the radiation of dipole antennas immediately above the earth's surface.³⁴ The same principle was used to determine the orientation of single molecules at an interface by their fluorescence lifetimes.³⁵ In evaporated Alq₃ films, the molecular orientation is random, thus the ensemble average of the dipole orientation is isotropic, the decay rate is given simply by

$$W_{ISO} = 1/3W_{perpendicular} + 2/3W_{parallel} \quad (6)$$

where $W_{perpendicular}$ and $W_{parallel}$ refer to the decay rates of dipoles perpendicular or parallel to the metal surface. W_{ISO} is the decay rate of an ensemble of dipoles with isotropic average orientation. On the other hand, in polymer OLEDs, a preferred dipole orientation may exist due to spin-coating of the polymer layer.^{13,36,37} The energy transfer to the metal cathode can be thought of as damping of the electric field in the cathode, so aluminum, with the highest reflectivity among the three materials gives rise to the least W_{ET} , and conversely magnesium gives rise to the largest (Figure 5). For all three cathodes, W_{ET} is drastically reduced for dipole-cathode distance above 60-80 nm. $(W_R + W_{ET})/W_0$ approaches 1.3 – 1.5 for a dipole-cathode distance of 80 – 140 nm. The dipole-cathode energy transfer is not negligible in this region since the dipole-cathode distance is still much less than the wavelength, but it no longer dominates the total decay rate. The sum of W_R and W_{ET} and their relative contributions depend sensitively on the exact microcavity structure.

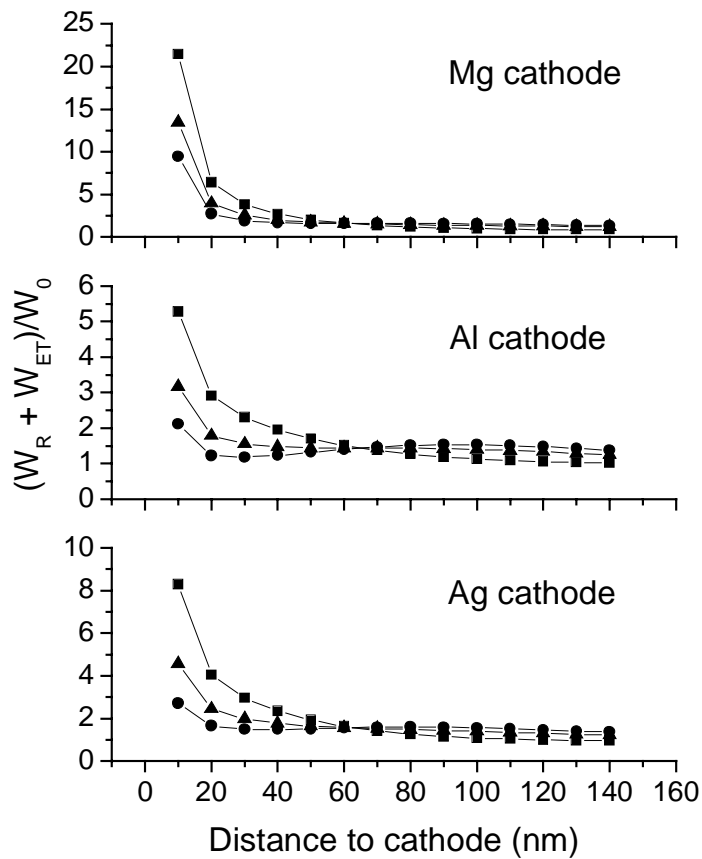


Figure 5 Decay rate due to the total electromagnetic fields of the dipole $(W_R + W_{ET})/W_0$ as a function of the dipole-cathode distance for three different cathode materials. Squares: perpendicular dipole, circles: parallel dipole, triangle: isotropic dipole. The OLED cavity has the structure: cathode/organics ($n = 1.7$, $t = 150\text{nm}$)/ITO ($n = 1.8$, $t = 120\text{ nm}$)/glass ($n=1.51$). Calculated for a monochromatic emitter at 524 nm.

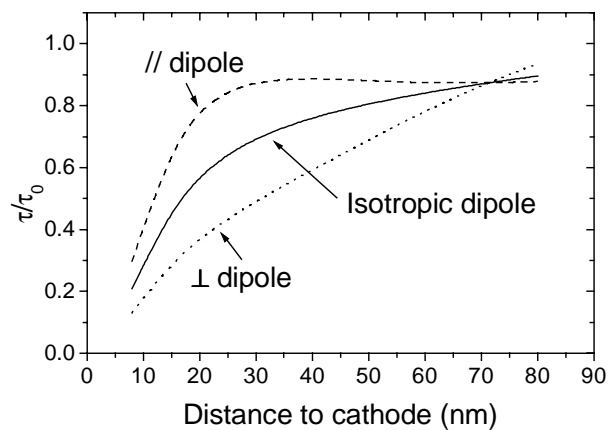


Figure 6 Normalized lifetime vs. exciton distance to cathode in the OLED (soda lime glass/100 nm ITO/40 nm PVK/80nm Alq₃/Ag).

The normalized lifetime, $\tau / \tau_0 = W_0 / W_{TOT}$, is plotted in Figure 6 as a function of the dipole-cathode distance and the dipole orientation for the OLED fabricated. Here W_{ET} decreases rapidly with increasing dipole-cathode distance and the lifetime levels off to approximately 90% of the intrinsic lifetime at a dipole-cathode separation of 80 nm (cf. Ref. 22).

2.5 Selected numerical results

The results of the CCQMM model are significant departures from the classical theory as illustrated in the radial plot of modal intensity vs. the mode angle in Alq₃. Figure 7a depicts the classical model, in which the TE and TM radiations are identical and isotropic, and the modes are delineated by the critical angles for TIR at the glass/air and ITO/glass interfaces. The total emitted flux is given by

$$F = 2\pi \int I(\theta) \sin \theta d\theta \quad (7)$$

for and angular intensity pattern, $I(\theta)$. The emission at large angles to normal is heavily weighted because of the large solid angles corresponding to large θ , so much so that 47% of the emitted light is in the ITO/organic modes according to ray optics. In reality, the cut-off wavelength of the thin ITO/organic waveguiding slab may fall within the visible region, and the strength of the ITO/organic modes are in general less than what the classical theory leads one to believe.

The results of the CCQMM microcavity model for a device with an 80-nm-thick Alq₃ layer at the peak emission wavelength ($\lambda = 524$ nm) is shown in Figure 7b. The exciton is assumed to be residing at the PVK/Alq₃ interface which is in close proximity to the antinode in the electric field at which point the TE and antinodal TM emissions are maximized (Figure 4). The radiation pattern retains much of the characteristics of that of an in-plane dipole again due to the fact that the electric field vector of both the TE and the antinodal TM waves are in the x-y plane.^{22, 42} The external and substrate modes form a continuum, because modal density is inversely proportional to the thickness of the region of space where the modes occupy. ITO/organic modes may exist at shorter wavelengths, but only as discrete modes. However, the energy in them may still be significant due to spatial confinement.

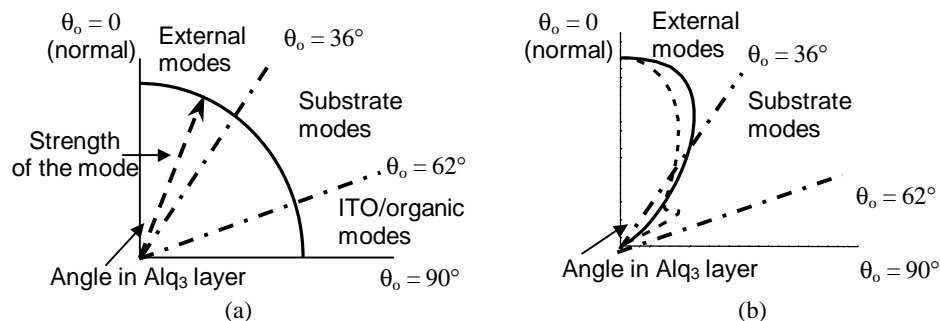


Figure 7 Radial plots of modal strength (intensity) vs. mode angle in Alq₃: (a) classical ray optics, (b) CCQMM model for an OLED with the structure: soda lime glass/100 nm ITO/40 nm PVK/80nm Alq₃/cathode. In (b), solid line: TE emission, dashed line: TM emission, the wavelength is 524 nm. The emitting center is assumed to be located at the PVK/Alq₃ interface.

3. EXPERIMENTAL

ITO-coated soda lime glass substrates ($n_{ITO} = 1.8$, $t_{ITO} \sim 165$ nm, Applied Films Corp.) were etched in a $HNO_3 : HCl : H_2O = 1 : 9 : 10$ solution at room temperature. Four substrates were etched for various amount of time where the etch rate was less than 10 nm/min. The resultant film thicknesses were measured by a Sloan Dektak III profilometer to be 165 nm, 135 nm, 95 nm and 80 nm, respectively. The colors of the specular reflection ($\sim 40^\circ$ from normal) from these substrates under a fluorescent light source as perceived by the unaided eye were purple, yellow, light yellow, and very pale purple, respectively. Bi-layer OLEDs were fabricated. The hole transport layer in all devices was a 40 nm layer of PVK, deposited by spin-coating from a PVK/chlorobenzene solution after the ITO surface was treated by an O₂ plasma.³⁸ The electron transport and emitting layer in all devices was Alq₃, deposited by vacuum sublimation at pressures $< 10^{-6}$ Torr. The deposition rate was

0.1-0.3 nm/s. The cathodes were 30-50 nm of Mg:Ag (10:1) followed by an Ag cap evaporated through a shadow mask. All devices were driven at a current density of 10 mA/cm². The luminance-current density-voltage characteristics of these OLEDs were measured by an HP4145B semiconductor parameter analyzer and a calibrated Si photodiode.

4. RESULTS AND DISCUSSION

The CCQMM model has been successfully applied to OLEDs to predict the spectrum,²² far-field intensity pattern, and edge emissions.^{6, 24, 41, 42} Moreover, the model accurately predicts the amount of increased external emission by the use of shaped, high-index-of-refraction substrates.^{6, 24, 42} In this section, we discuss the dependency of various efficiency measures on the thickness of the ITO anode (Figure 8a).

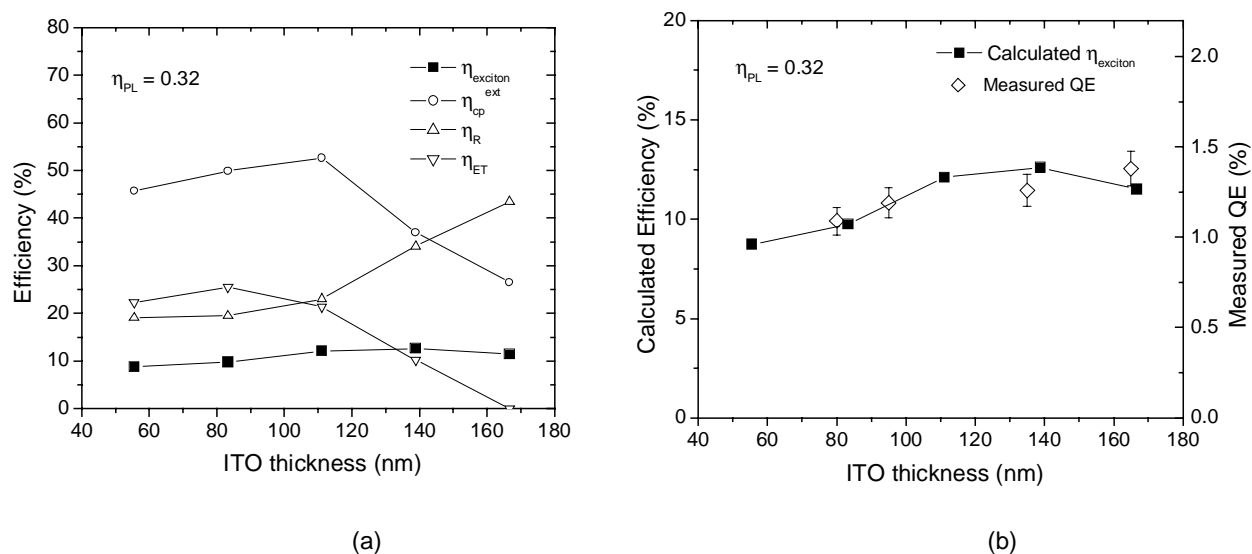


Figure 8 (a) Various efficiencies vs. ITO thickness calculated for OLEDs with the structure: soda lime glass/ITO ($n = 1.8$)/40 nm PVK/80 nm Alq₃/Ag. Closed squares: $\eta_{exciton}$, open circles: η_{cp}^{ext} , open up triangles: η_R , and open down triangles: η_{EL} . $\eta_{PL} = 0.32$ is used in the calculations. The lines are guides to the eye only. (b) Comparison of the calculated $\eta_{exciton}$ (squares) and the measured external quantum efficiency (diamonds) as a function of ITO thickness.

The efficiencies are calculated for three material systems with $\eta_{PL} = 0.32$. The external coupling efficiency, η_{cp}^{ext} , is independent of the non-radiative processes, thus is also independent of η_{PL} , and a peak value of 52.6 % is observed at an ITO thickness of 110 nm. But calculation of the distribution into the three radiative modes reveals that the suppression of ITO/organic modes due to the thinness of the ITO layer also plays a role.^{41, 42} As the ITO thickness increases above 110 nm, the ITO/organic modes start to contribute to the radiative decay and η_{cp}^{ext} decreases rapidly. However, the more relevant parameter to device optimization is the number of photons emitted externally per singlet exciton, $\eta_{exciton}$, which is a product of η_{cp}^{ext} and η_R . The total decay rate, W_{TOT} , does not change appreciably with the change in the thickness of the ITO layer; however, the relative strength of the radiative decay and the dipole-cathode energy transfer depends sensitively on the ITO thickness. With a thicker ITO, the increase in the rate of radiative decay W_R , together with the decrease in dipole-cathode energy transfer W_{ET} , causes η_R to increase faster than the decrease in η_{cp}^{ext} , resulting in a notable increase in $\eta_{exciton}$. 138 nm of ITO gives the most efficient device on planar substrates where 12.6% of the singlet excitons emit a photon externally, whereas the device on 55 nm ITO is over 30% less efficient at $\eta_{exciton} = 8.7\%$.

The dependence of device efficiency variation with ITO thickness was measured (Figure 8b). The experimental data showed a monotonic increase with ITO layer thickness from an external quantum efficiency of 1.1% with 55 nm of ITO to 1.4% with

165 nm of ITO. The fact that the device on 165 nm ITO is more efficient than the one on 135 nm ITO can be attributed to measurement uncertainties and the slight scattering of substrate modes which are more intense in the device with 165 nm ITO.⁴²

5. CONCLUSIONS

We used a CCQMM model to describe the recombination of excitons in an OLED. Microcavity effects on both the radiative modes and the dipole-cathode energy transfer are discussed. The dipole-cathode energy transfer was calculated for several common cathode materials and differences were found. Excitons located less than 60 nm away from the cathode were found to suffer from a high rate of energy transfer (cathode quenching). $\eta_{exciton}$, defined as the external photons emitted by an exciton of the appropriate type, is offered as a measure to be maximized for optimizing the external coupling efficiency of the OLED. The numerical results agreed qualitatively with the experimental data from OLEDs with various ITO anode thicknesses. The calculated value of $\eta_{exciton}$ should facilitate determination of the ratio of singlet/triplet excitons in OLEDs, which is a subject of ongoing investigation.

ACKNOWLEDGEMENTS

This work was supported by the New Jersey Commission on Science and Technology (NJCST) and the Defense Advanced Research Project Agency (DARPA).

REFERENCES

1. B. E. A. Saleh and M. C. Teich, *Fundamentals of Photonics*, Wiley, New York, 1991.
2. N. C. Greenham, R. H. Friend, and D. D. C. Bradley, "Angular dependence of the emission from a conjugated polymer light-emitting diode: implications for efficiency calculations", *Adv. Mater.* **6**, pp. 491-493, 1994.
3. T. Tsutsui, "Progress in electroluminescent devices using molecular thin films", *Mater. Res. Bull.* **22**, pp.39-45, 1997.
4. J. Kido and Y. Iizumi, "Fabrication of highly efficient organic electroluminescent devices", *Appl. Phys. Lett.* **73**, pp. 2721-2723, 1998.
5. T. Tsutsui, M.-J. Yang, M. Yahiro, K. Nakamura, T. Wantanabe, T. Tsuji, Y. Fukuda, T. Wakimoto, and S. Miyaguchi, "High quantum efficiency in organic light-emitting devices with iridium-complex as a triplet emissive center", *Jpn. J. Appl. Phys.* **38**, pp. L1502-L1504, 1999.
6. M.-H. Lu, C. F. Madigan, and J. C. Sturm, "Experiment and modeling of conversion of substrate-waveguided light to surface-emitted light", *Mat. Res. Soc. Symp. Proc.* **621**, pp. Q3.7.1-Q3.7.6, 2000.
7. S. Saito, T. Tsutsui, M. Erra, N. Takada, C. Adachi, Y. Hamada, and T. Wakimoto, "Progress in organic multilayer electroluminescent devices", *Proc. SPIE* **1910**, pp. 212-221, 1993.
8. V. Cirmova and D. Neher, "Microcavity effects in single-layer light-emitting devices based on poly(*p*-phenylene vinylene)", *J. Appl. Phys.* **79**, pp. 3299-3306, 1996.
9. D. G. Lidzey, M. A. Pate, D. M. Whittaker, D. D. C. Bradley, M. S. Weaver, A. A. Fisher, and M. S. Skolnick, "Control of photoluminescence emission from a conjugated polymer using an optimised microcavity structure", *Chem. Phys. Lett.* **263**, pp. 655-660, 1996.
10. J. Gruner, F. Cacialli, and R. H. Friend, "Emission enhancement in single-layer conjugated polymer microcavities", *J. Appl. Phys.* **80**, pp. 207-215, 1996.
11. H. F. Wittman, J. Gruner, R. H. Friend, G. W. C. Spencer, S. C. Moratti, and A. B. Holmes, "Microcavity effect in a single-layer polymer light-emitting diode", *Adv. Mater.* **7**, pp. 541-544, 1995.
12. H. Becker, S. E. Burns, and R. H. Friend, "Effect of metal films on the photoluminescence and electroluminescence of conjugated polymers", *Phys. Rev. B*, **56**, pp. 1893-1905, 1997.
13. J.-S. Kim, P. K. H. Ho, N. C. Greenham, and R. H. Friend, "Electroluminescence emission pattern of organic light-emitting diodes: implications for device efficiency calculations", *J. Appl. Phys.* **88**, pp. 1073-1081, 2000.
14. R. R. Chance, A. Prock, and R. Sibley, "Molecular Fluorescence and energy transfer near interfaces", *Adv. Chem. Phys.*, **37**, pp. 1-65, 1978.
15. R. R. Chance, A. Prock, and R. Silby, "Comments on the classical theory of energy transfer", *J. Chem. Phys.* **62**, pp. 2245-2253, 1975.
16. R. R. Chance, A. H. Miller, A. Prock, and R. Silby, "Fluorescence and energy transfer near interfaces: the complete and quantitative description of the Eu³⁺/mirror systems", *J. Chem. Phys.* **63**, pp. 1589-1595, 1975.
17. K. B. Kahen, "Optical modeling of organic light-emitting diode multilayer device structures", *Mat. Res. Soc. Symp.* **660**, pp. JJ4.2.1-JJ4.2.6, 2001.
18. A. L. Burin and M. A. Ratner, "Exciton migration and cathode quenching in organic light emitting diodes", *J. Phys. Chem. A* **104**, pp. 4704-4710, 2000.

19. K. Ujihara, "Quantum theory of a one-dimensional optical cavity with output coupling. Field quantization", *Phys. Rev. A* **12**, pp. 148–158, 1975.
20. D. G. Deppe and C. Lei, "Spontaneous emission from a dipole in a semiconductor microcavity", *J. Appl. Phys.* **70**, pp. 3443-3448, 1991.
21. G. Bjork, S. Machida, Y. Yamamoto, and K. Igeta, "Modification of spontaneous emission rate in planar dielectric microcavity structures", *Phys. Rev. A* **44**, pp. 669-681, 1991.
22. V. Bulovic, V. B. Khalfin, G. Gu, P. E. Burrows, D. Z. Garbuzov, and S. R. Forrest, "Weak microcavity effects in organic light-emitting devices", *Phys. Rev. B*, **58**, pp. 3730-3740, 1998.
23. C. F. Madigan, M.-H. Lu, and J. C. Sturm, "Improvement of output coupling efficiency of organic light emitting diodes by backside substrate modification", *Appl. Phys. Lett.* **76**, pp. 1650-1652, 2000.
24. M.-H. Lu, C. F. Madigan, and J. C. Sturm, "Improved external coupling efficiency in organic light-emitting devices on high-index substrate", *IEDM Tech. Dig.*, pp. 600-603, 2000.
25. T. Yamasaki, K. Sumioka, and T. Tsutsui, "Organic light-emitting device with an ordered monolayer of silica microspheres as a scattering medium", *App. Phys. Lett.* **76**, pp. 1243-1245, 2000.
26. M. Pope and C. E. Swenberg, *Electronic Processes in Organic Crystals*, Oxford University Press, Oxford, 1982.
27. D. Z. Garbuzov, V. Bulovic, P. E. Burrows, and S. R. Forrest, "Photoluminescence efficiency and absorption of aluminum-tris-quinolate (Alq₃) thin films", *Chem. Phys. Lett.* **249**, pp. 433-437, 1996.
28. Y. Cao, I. D. Parker, G. Yu, C. Zhang, and A. J. Heeger, "Improved quantum efficiency for electroluminescence in semiconducting polymers", *Nature* **397**, pp. 414-417, 1999.
29. G. Gu, D. Z. Garbuzov, P. E. Burrows, S. Venkatesh, and S. R. Forrest, "High-external-quantum-efficiency organic light-emitting devices", *Opt. Lett.* **22**, pp. 396-398, 1997.
30. A. A. shoustikov, Y. You, and M. E. Thompson, "Electroluminescence color tuning by dye doping in organic light-emitting diodes", *IEEE J. Sel. Top. Quan. Elec.* **4**, pp. 3-13, 1998.
31. E. Hecht, *Optics*, 3rd ed. (Addison-Wesley, Reading Mass. 1998).
32. C. W. Tang, S. A. van Slyke, and C. H. Chen, "Electroluminescence of doped organic thin films", *J. Appl. Phys.* **65**, pp. 3610-3616, 1989.
33. C. T. Tai, *Dyadic Green's Function in Electromagnetic Theory*, Intext, New York, 1971.
34. A. Sommerfeld, *Electrodynamics*, Academic Press, New York, 1952.
35. J. J. Macklin, J. K. Trautman, T. D. Harris, and L. E. Brus, "Imaging and time-resolved spectroscopy of single molecules at an interface", *Science* **272**, pp. 255-258, 1996.
36. Y. Shi, J. Liu, and Y. Yang, "Device performance and polymer morphology in polymer light emitting diodes: The control of thin film morphology and device quantum efficiency", *J. Appl. Phys.* **87**, pp. 4254-4263, 2000.
37. J. Liu, Y. Shi, L. Ma, and Y. Yang, "Device performance and polymer morphology in polymer light emitting diodes: The control of device electrical properties and metal/polymer contact", *J. Appl. Phys.* **88**, pp. 605-610, 2000.
38. C.-C. Wu, C.-I. Wu, J. C. Sturm, and A. Kahn, "Surface modification of indium tin oxide by plasma treatment: An effective method to improve the efficiency, brightness and reliability of organic light emitting devices", *Appl. Phys. Lett.* **70**, pp. 1348-1350, 1997.
39. The results presented in figures 6 and 8 are based on the lifetime calculated for each specific OLED rather than using the total decay rate calculated in Ref. 22. Thus they are more accurate than previously published results in Refs. 6 and 24, although the difference is small.
40. H. Aziz, Z. D. Popovic, N.-X. Hu, A.-M. Hor, and G. Xu, "Degradation mechanism of small molecule-based organic light-emitting devices", *Science* **283**, pp. 1900-1902, 1999.
41. M.-H. Lu and J. C. Sturm, "External coupling efficiency in planar organic light emitting devices", *Appl. Phys. Lett.*, **78**, pp. 1927-1929, 2001.
42. M.-H. Lu and J. C. Sturm, "Optimization of External Coupling and Light Emission in Organic Light-Emitting Devices: Modeling and Experiment", *J. Appl. Phys.* **91**, pp. 595-604, 2002.